JOURNAL OF CATALYSIS **178,** 275–283 (1998)
ARTICLE NO. CA982135

Kinetics of CO and CO_2 Evolution During the Temperature-Programmed Oxidation of Coke Deposited on Cracking Catalysts

Chao'en Li, Cam Le Minh, and Trevor C. Brown[1]

Division of Chemistry, University of New England, Armidale, NSW, Australia

Received November 18, 1997; revised March 31, 1998; accepted April 28, 1998

The reaction kinetics of evolved carbon monoxide and carbon dioxide during the temperature programmed oxidation (TPO) of an industrially spent fluid cracking catalyst have been investigated. Two pathways to CO and two to CO_2 evolution, all involving either undissociated or dissociated surface oxide complexes, were assumed. Rate coefficient parameters and O_2 reaction orders were then optimized to simulate the TPO profiles recorded over a range of conditions: heating rates of 2, 5 and 10°C and O_2 partial pressures of 0.939, 1.11, and 5.0% in an atmosphere of N_2. Evolution rates of CO during TPO are independent of the O_2 partial pressure, whereas an order of 0.75 is indicated for CO_2 formation. Because of differences in assumed mechanisms and carbon substrates, calculated preexponential factors and activation energies can not be readily compared with literature values, although some comparisons are made. If the heating rate is high (≥ 5°C min^{-1}) and the oxygen partial pressure is low ($\leq 1\%$), the shape of TPO profiles for highly saturated hydrocarbon coke deposited on cracking catalyst are affected by changes in the rate-determining step with increasing temperature.

INTRODUCTION

The technique of temperature-programmed oxidation (TPO) with either evolved-gas or gravimetric analysis is often employed to investigate coke deposited on catalysts. Details of the proximity of coke to metal and nonmetal sites or the nature of coke are then inferred from the position of peaks in the resultant TPO profiles. The shape of these profiles can also be affected by coke particle size and morphology (1). Recently, we have shown that the temperature-dependence of the coke combustion mechanism can also affect the shape of the evolved CO and CO_2 TPO profiles (2).

Information on catalytic coke combustion mechanisms is limited. Two factors have been shown to affect the apparent kinetics: (i) combustion within the catalyst pores can, under certain conditions, be diffusion limited (3–5), and (ii) oxidation of the hydrogen component of coke, which precedes the carbon combustion, results in significant temperature fluctuations (3, 6–8). The latter is a particular problem for hydrogen-rich coke. Perhaps as a consequence of these factors, the individual steps involved in CO and CO_2 evolution during coke combustion have not been investigated in depth. However, much research has been carried out, and many conflicting mechanisms have been reported on amorphous carbon and coal char combustion. Despite the confusion, there is overwhelming evidence that surface-oxides are important precursors to both CO and CO_2 formation. The stoichiometry and mechanism of CO formation at low temperatures has recently been determined by simultaneously monitoring the weight changes and evolved gases during oxygen exposure to amorphous carbons and during subsequent temperature-programmed desorption (9, 10). Three elementary steps represent the heterogeneous elimination of CO during carbon oxidation:

$$^*C + O_2 \rightleftharpoons {}^*C + (O_2), \quad [1]$$

$$^*C(O_2) \rightarrow {}^*C(O) + CO, \quad [2]$$

$$^*C(O) \rightarrow CO. \quad [3]$$

Here, $^*C$ is a free carbon site, $^*C(O_2)$ is a dioxygen surface complex, and $^*C(O)$ is a stable oxygen surface species. This mechanism indicates two pathways to CO, hence two rate expressions. For CO_2 evolution, two pathways may also be assumed involving the two oxygen surface complexes formed via Reactions [1] and [2] (9):

$$^*C + O_2 \xrightarrow{^*C(O_2)} CO_2 \quad [4]$$

and

$$^*C + O_2 \xrightarrow{^*C(O)} CO_2. \quad [5]$$

In this paper, TPO of an industrial spent cracking catalyst is used to investigate the kinetics of coke combustion and the effect these kinetics have on the shape of the TPO profiles. Typically, cracking catalysts consist of a USY zeolite in an active alumina, silica–alumina, clay, and rare-earth oxide matrix. The majority of the coke deposited on

[1] To whom correspondence should be addressed. Telephone: +61 2 6773 2872. Fax: +61 2 6773 3268. E-mail: tbrown3@metz.une.edu.au.

0021-9517/98 $25.00

this catalyst consists of highly unsaturated hydrocarbons. To describe the oxidation kinetics of this type of coke, a single-site model is developed.

EXPERIMENTAL

The apparatus constructed to monitor CO and CO_2 evolution continuously during oxidation has been previously described in detail (2). A recent addition to this equipment is a hygrometer situated between the reactor and the carbon oxide detectors. This Model 95A Super Dry Hygrometer (Alpha Moisture Systems) records the ambient dew point over the range 0 to −80°C which corresponds to water vapor pressures of 6000 to 0.5 ppm. It is calibrated by decomposing accurately weighed quantities of $Ca(OH)_2$ (>98% BDH). Carbon oxides produced during a linear temperature-programmed oxidation of coke are split into two streams. The first is mixed with hydrogen and then flows through a ruthenium catalyst where complete conversion of both CO and CO_2 to methane occurs. The partial pressure of methane is then quantitatively analyzed by a flame ionization detector (FID). For the second stream, CO_2 is removed by passing through ascarite (Aldrich), whereas CO passes unhindered and is mixed with H_2, converted to methane over ruthenium, and analyzed by a second FID. CO_2 partial pressure is then the difference between the two FID responses. Both signals are calibrated using CO and CO_2 standards (119 ± 2 ppm CO in N_2 and 519 ± 10 ppm CO_2 in N_2). Reactor temperatures and resultant carbon oxide partial pressures are transferred to a personal computer by means of Strawberry Tree's data acquisition hardware and software. Conversion of partial pressures p_{FID} (ppm) to carbon oxide and water evolution rates [μmoles (g of catalyst)$^{-1}$ °C^{-1}] involves consideration of the molar flow rate $\dot{n}$ (moles min^{-1}) and the weight of catalyst w_{cat}. Further calibration is required to take into account the reaction temperature and effective pumping rate S (11, 12). The rate of CO, CO_2, and H_2O evolution is

$$\text{Rate } [\mu\text{mole (g of cat.)}^{-1}\,^{\circ}\text{C}] = \frac{2 \times p_{\mathrm{FID}}(\text{ppm}) \times p_{\mathrm{Total}}(\text{atm}) \times \dot{n} \times S}{w_{\mathrm{cat}} \times \beta \times R \times T}.$$

R is the gas constant, β is the linear heating rate, and p_{Total} is the pressure in the vicinity of the coked catalyst, which was determined to be 1.2 atm for all experiments. Effective pumping speeds were estimated by adjusting S so that total carbon equaled the carbon measured using a Carlo Erba CHNS-O elemental analyzer [i.e., for the spent catalyst analyzed in this work wt% C = 0.84% g (g of catalyst)$^{-1}$]. Values of S were found to be weakly dependent on the heating rate; $1.1 \pm 0.1 \times 10^3$ μmoles L^{-1} for 2°C min^{-1}, $0.95 \pm 0.04 \times 10^3$ μmoles L^{-1} for 5°C min^{-1} and $0.93 \pm 0.05 \times 10^3$ μmoles L^{-1} for 10°C min^{-1}. The effective pumping speed for passage of H_2O to the hygrometer at a heating rate of 5°C min^{-1} was calculated to be $0.94 \pm 0.5 \times 10^3$ μmoles L^{-1}.

In addition to three heating rates, three oxygen partial pressures were employed—0.939 ± 0.002%, 1.11 ± 0.01% and 5.0 ± 0.2% all dilute in N_2. Gases were supplied and analyzed by BOC Gases. The spent cracking catalyst was taken from the output of the catalytic cracker at the Ampol Refinery, Lytton, Queensland, Australia. The N_2 BET surface area of this substrate is 105 ± 5 m^2 g^{-1}. The Si/Al ratio of the spent catalyst is 2.3 as determined by X ray fluoresence (XRF). Other elements detected by XRF are Ti (1.0 wt%), La (1.0 wt%), Nd (0.3 wt%), Fe (5600 ppm), Ni (1544 ppm), Zn (265 ppm), and V (543 ppm). The total carbon deposited on the spent catalyst is 0.84 ± 0.04 g%/g of catalyst as determined both by a Carlo Erba CHNS-O elemental analyzer and by a quantitative analysis of the carbon oxide profiles during TPO.

EXPERIMENTAL RESULTS

The shapes of TPO profiles and the effect of altering heating rates has been described previously (2, 13). Figure 1 illustrates the TPO evolved CO, CO_2, and H_2O profiles obtained for the industrial spent cracking catalyst in 0.939% O_2 with a heating rate of 10°C min^{-1}. Carbon monoxide evolution shows a single symmetric peak for all heating rates and oxygen partial pressures, although the height of

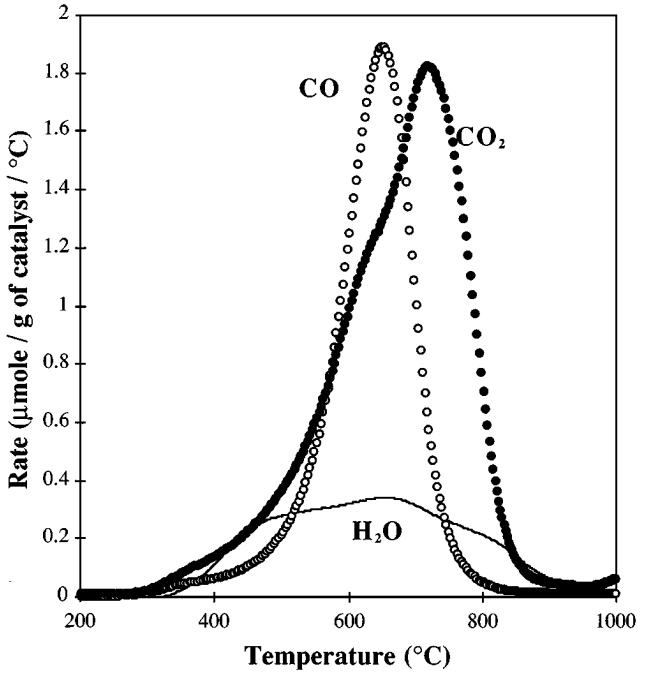

FIG. 1. Experimental evolution rates of CO (○), CO_2 (●), and H_2O (–) during TPO of a spent cracking catalyst in 0.939% O_2 with a heating rate of 10°C/min.

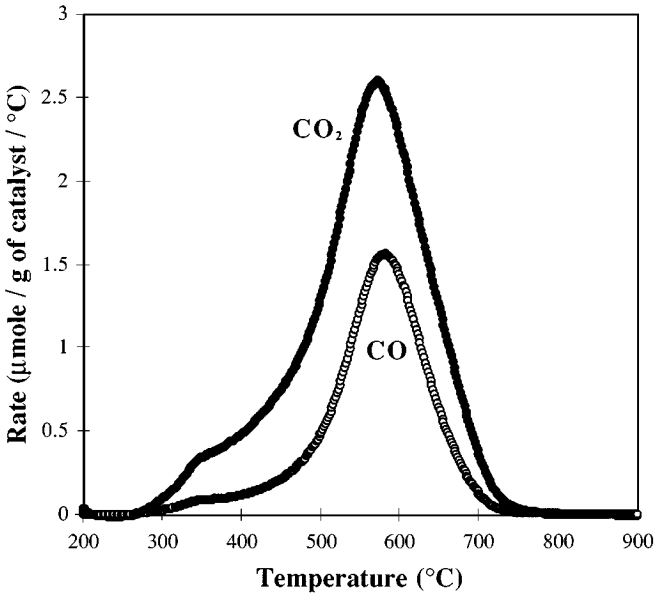

FIG. 2. Experimental evolution rates of CO (○), and CO_2 (●) during TPO of a spent cracking catalyst in 0.939% O_2 with a heating rate of 5°C/min.

this peak is substantially decreased in the 5% O_2 TPO (Fig. 2). At 10°C min^{-1}, carbon dioxide evolution has a shoulder at ca. 620°C and a maximum rate at ca. 725°C, whereas at 5°C min^{-1}, this shoulder and peak are reversed (Fig. 3b). In 5% O_2, CO_2 formation dominates. Low levels of H_2O evolution relative to carbon oxide formation, as shown in Fig. 1, are indicative of aromatic coke or highly unsaturated hydrocarbons. The overall H/C ratio is 0.42, which is clearly too small for alkane or simple alkene components. Because of such low levels of hydrogen, the overall apparent reactivity is assumed, in the kinetic analysis, to be independent of this element. In addition, H_2O evolution beyond 850°C is higher than the combined CO and CO_2 rates, indicating that adsorption on the reactor walls is affecting the intrinsic kinetics. As a consequence, the H_2O rates have not been modeled.

KINETIC MODEL FOR CARBON OXIDE EVOLUTION

A single-site kinetic model is developed to describe the observed structure of evolved carbon oxides during TPO of coke consisting of highly unsaturated hydrocarbons. That is, all carbons associated with this type of coke are taken to be equivalent.

The first step upon exposure of the coked catalyst to oxygen is the formation of undissociated surface oxide complexes (Reaction [1]). This initial exposure occurs at low temperatures (200°C) when evolved carbon oxide species are not observed. Under these conditions, the exothermic formation of $^*C(O_2)$ should not have as great an impact on the substrate temperature as occurs at higher temperatures when the loss of translational energy upon adsorption is significant. Also the choice of a spent catalyst with a high unsaturated hydrocarbon content was to ensure that hydrogen oxidation and hence temperature fluctuations are minimized. The temperature recorded by the thermocouple situated adjacent to the catalyst is therefore taken to be the temperature of the catalyst. We also assume that at the lowest temperatures, before evolution of any carbon

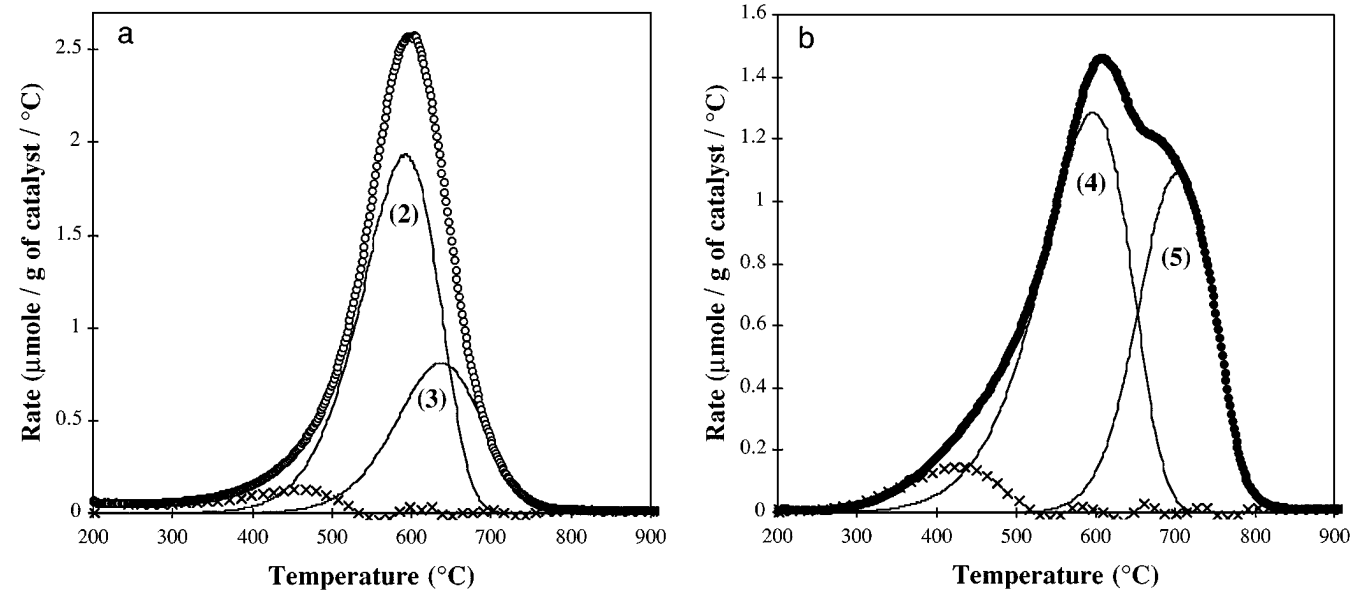

FIG. 3. Experimental evolution rates of (a) CO and (b) CO_2 during TPO of a spent cracking catalyst in 0.939% O_2 with heating rate of 5°C/min. Lines under the TPO profiles represent simulated peaks associated with Reactions [2]–[5]. Crosses are the difference between experimental and model data.

oxides, the surface becomes saturated with undissociated oxide complexes. That is, the concentration of oxygen on the carbon or catalyst surface and the equilibrium between molecular oxygen complexes and free oxygen is independent of the oxygen partial pressure. The metastable oxide complexes which form are the Type A species described by Brown *et al.* (10). As a consequence, the concentration of $^*C(O_2)$ may be set equal to the concentration of $^*C$. This also means that temperature fluctuations at all temperatures, high as well as low, during TPO should be minimal because exothermic adsorption steps are negligible at high temperatures.

Carbon monoxide evolution then occurs via the undissociated surface oxide complex which rearranges to form a stable surface oxide [$^*C(O)$] and CO (Reaction [2]). The stable surface oxide may then desorb (Reaction [3]) and hence also contribute to measured carbon monoxide. By assuming that the rate-determining steps are a rearrangement of the complex for Reaction [2] and a direct desorption for Reaction [3], then the total temperature-dependent rate of CO evolution is

$$\frac{d[CO]}{dT} = \frac{k_2}{\beta}[^*C(O_2)]p_{O_2}^{n_2} + \frac{k_3}{\beta}[^*C(O)]p_{O_2}^{n_3} = \frac{k_2}{\beta}[^*C]p_{O_2}^{n_2} + \frac{k_3}{\beta}[^*C(O)]p_{O_2}^{n_3}. \quad [6]$$

Hence n_2 and n_3 are the orders with respect to the oxygen pressure but are predicted to be zero order, and hence both rate coefficients are unimolecular.

Formation of CO_2 proceeds via either the undissociated surface oxide complex or the dissociated surface oxides produced in Reaction [2]. Reactions [4] and [5] both indicate CO_2 forms following interaction between the respective surface oxides and molecular oxygen. The total rate of CO_2 evolution is therefore given by

$$\frac{d[CO_2]}{dT} = \frac{k_4}{\beta}[^*C(O_2)]p_{O_2}^{n_4} + \frac{k_5}{\beta}[^*C(O)]p_{O_2}^{n_5} = \frac{k_4}{\beta}[^*C]p_{O_2}^{n_4} + \frac{k_5}{\beta}[^*C(O)]p_{O_2}^{n_5}. \quad [7]$$

The orders with respect to oxygen ($n_2 - n_5$) for Reactions [2]–[5] are determined later by simulating the TPO data obtained under different partial pressures of O_2.

Model Parameters

The temperature-dependent carbon concentration [$^*C(T_j)$] is calculated by subtracting the available carbon which has been oxidized via Reactions [2] and [4] from the initial concentration of carbon sites [$^*C_0$], as shown by

$$[^*C(T_j)] = [^*C_0] - 2 \times \sum_{i=1}^{j} \frac{k_2}{\beta}[^*C(T_{i-1})]p_{O_2}^{n_2}\Delta T - \sum_{i=1}^{j} \frac{k_4}{\beta}[^*C(T_{i-1})]p_{O_2}^{n_4}\Delta T. \quad [8]$$

Carbon concentrations on the right-hand side of Eq. [8] are the totals calculated following the preceding temperature increment. The sum of the rates of CO evolution via Reaction [2] must be multiplied by 2 because two carbons are lost for each observed CO; one forms the stable surface oxide [$^*C(O)$].

The only source of [$^*C(O)$] in the entire combustion process is assumed to be via Reaction [2]. For each CO produced by this reaction step, one $^*C(O)$ forms, and this concentration is reduced by subtracting the sum of the rates of Reactions [3] and [5] multiplied by the temperature increment. Hence the temperature-dependent concentration of stable surface oxides is given by

$$[^*C(O)(T_j)] = \sum_{i=1}^{j} \frac{k_2}{\beta}[^*C(T_{i-1})]p_{O_2}^{n_2}\Delta T - \sum_{i=1}^{j} \frac{k_3}{\beta}[^*C(O)(T_{i-1})]p_{O_2}^{n_3}\Delta T - \sum_{i=1}^{j} \frac{k_5}{\beta}[^*C(O)(T_{j-1})]p_{O_2}^{n_5}\Delta T. \quad [9]$$

An obvious constraint on Eq. [9] is that the total concentration of stable surface oxides is equal to zero when all coke has been removed, that is, $[^*C(O)(T_j)] = 0$ when the rate of carbon-oxide evolution becomes zero. In all TPO profiles, the area under the peak corresponding to Reaction [2] is greater than the area associated with Reaction [5]. Hence, Reaction [3] has been introduced to ensure a mass balance of stable surface oxides is achieved.

By replacing rate coefficients in Eqs. [6] and [7] with Arrhenius expressions, evolved CO and CO_2 rate equations become

$$\frac{d[CO]}{dT} = \frac{A_2}{\beta}\exp\left(\frac{-E_2}{RT}\right)[^*C]p_{O_2}^{n_2} + \frac{A_3}{\beta}\exp\left(\frac{-E_3}{RT}\right)[^*C(O)]p_{O_2}^{n_3} \quad [10]$$

and

$$\frac{d[CO_2]}{dT} = \frac{A_4}{\beta}\exp\left(\frac{-E_4}{RT}\right)[^*C]p_{O_2}^{n_4} + \frac{A_5}{\beta}\exp\left(\frac{-E_5}{RT}\right)[^*C(O)]p_{O_2}^{n_5}. \quad [11]$$

The complete rate equations follow when eqs. [8] and [9] are substituted into eqs. [10] and [11]. TPO-evolved carbon oxide data may be simulated by adjusting nine parameters; $\log A_2$, E_2, $\log A_3$, E_3, $\log A_4$, E_4, $\log A_5$, E_5, and $[{}^*C_0]$. The unit used in the calculations for partial pressure of oxygen is the percentage of the O_2 in the nitrogen as reported by the manufacturer. Hence the units of the preexponential factors are $\text{min}^{-1}\ \%O_2^{-n}$, where n is the O_2 order. Structure in the evolved gas profiles, particularly the CO_2 curve, and data obtained at different heating rates provide sufficient independent information to allow an accurate determination of the nine parameters.

Following optimization of the nine parameters using the 0.939% O_2 data, the order of the O_2 partial pressure for each of the four reactions [2]–[5] was determined by simulating the experimental TPO curves obtained using the higher partial pressure of oxygen. The best-fit rate parameters calculated for the low O_2 pressure profiles were held constant for the 1.11 and 5% O_2 data, and only the four orders with respect to O_2 (i.e., for Reactions [2]–[5]) and the free carbon concentration were optimized.

Minimization Procedures

The Solver module within Excel 5 was used to optimize all parameters. This module performs nonlinear least-squares curve fitting and applications to kinetic systems have been reported in the literature (14, 15). For each TPO, four columns of modeled rates, corresponding to two sources of CO (Eq. [10]) and two for CO_2 evolution (Eq. [11]) are listed adjacent to the two columns of experimental data and temperatures in an Excel spreadsheet. Two columns of data representing the temperature-dependent coke and stable surface oxides are also listed. The sum of the squares of the difference between experimental rates and model values is then minimized, using the Solver module, by adjusting the parameters. The constraint that Eq. [9] is zero when all carbon has been removed is incorporated into the minimized value by adding the square of Eq. [9] calculated at the final temperature.

Errors are not automatically calculated by the Excel Solver module, but methodology suggested by Billo (15) has been adapted to determine the standard deviation for all optimized parameters. The procedure ultimately used to optimize the Arrhenius parameters was to simultaneously model six TPO-evolved CO and CO_2 profiles recorded with heating rates of 5°C/min and 10°C/min in an oxygen partial pressure of 0.939%. For the 1.11 and 5% O_2 partial-pressure TPO profiles, the 0.939% O_2 optimized rate parameters were used, and the oxygen orders varied to fit the data. Reported errors are, for the Arrhenius parameters, calculated standard deviations from the 0.939% O_2 data, and for the orders calculated standard deviations from the 1.11 and 5% O_2 pressure profiles.

TABLE 1

Optimized Rate Coefficient Parameters, O_2 Reaction Orders, and Total Carbon for Reactions [2] [5] Observed During the TPO of a Spent Cracking Catalyst [a]

Parameter	Value
CO evolution:	
$\log A_2$	6.4 ± 0.2
E_2 (kJ mol^{-1})	131 ± 5
n_2	0.16 ± 0.06
$\log A_3$	0.4 ± 0.2
E_3 (kJ mol^{-1})	36 ± 3
n_3	0.2 ± 0.2
CO_2 evolution:	
$\log A_4$	4.2 ± 0.3
E_4 (kJ mol^{-1})	98 ± 5
n_4	0.80 ± 0.06
$\log A_5$	7.0 ± 0.2
E_5 (kJ mol^{-1})	151 ± 3
n_5	0.7 ± 0.1
$[-C_0]$ (μmole g^{-1})	
Highly unsaturated coke	644 ± 5
Residual coke	56 ± 5

[a] Residual coke is the area consisting of the difference between the experimental and model data. The range of TPO conditions employed in the analysis were oxygen partial pressure 0.939–5% and heating rates of 2–10°C min^{-1}.

Model Results

Optimized parameters required to model evolved carbon oxide species during TPO of coke deposited on the spent cracking catalyst in 0.939% O_2 and with a heating rate of 5°C/min are listed in Table 1. Figure 3 illustrates the fit to the TPO of the spent catalyst in 0.939% O_2 and with a heating rate of 5°C/min.

A complication in the modeling is the small low-temperature peak in the TPO of catalytic coke which has been associated with nonaromatic coke or coke formed in the vicinity of metal sites. Alternatively, the exothermic formation of water from aromatic coke, which occurs at low temperatures (13), may cause a fluctuation in the catalyst temperature and cause the premature evolution of some of the aromatic coke. This peak, which represents less than 10% of the coke, is shown in Fig. 3 by the crosses, the difference between the experimental and the modeled data. In order to overcome this complication, the low-temperature experimental data which are affected by this peak are not included in the minimization. The temperature below which data were excluded depended on the heating rate and oxygen partial pressure but was in the range 500–550°C.

It was not possible to fit precisely the 10°C min^{-1} profiles at the highest oxidation temperatures. This is partially because the furnace was unable to maintain this high heating rate beyond 850°C. Also, however, under these conditions, the coke survives to higher temperatures where

restructuring of the catalyst would occur and so affect the rate of elimination of the coke. At a heating rate of 5°C min^{-1}, all coke has been removed by 820°C, and accurate simulations were possible. The catalyst generally experiences only temperatures up to 800°C in the regenerating unit of the cracker. As a consequence, only data measured up to 850°C were included in the minimization.

DISCUSSION

Rate Parameters and Reaction Orders

The most significant data listed in Table 1 are the activation energies and O_2 reaction orders. Interpretation of the observed preexponential factors are difficult because of the unknown order with respect to the carbon concentration and the unknown O_2 collision frequency within the catalyst. However, a comparison of the rate coefficient parameters obtained for the two CO_2 evolution peaks indicates agreement with the compensation effect (16). That is, the larger the preexponential factor, the larger the activation energy. This is also the case with the CO parameters for Reactions [2] and [3], but as discussed later the mechanism for Reaction [3] is uncertain.

Orders with respect to the O_2 partial pressure are informative. Both carbon monoxide evolution peaks proceed with a zero-order dependence, whereas both carbon dioxide rates depend on a 0.75 oxygen order. Zero-order reactions indicate that desorption is rate determining (17) and independent of the O_2 concentration, as was proposed in developing the rate expression Eq. [6]. Blyholder and Eyring (18) demonstrated that a 0.75-order process is an intrinsic half-order reaction with respect to oxygen but occurs inside the pores of the substrate. They were concerned with an apparent 0.75 order for CO evolution and concluded that oxygen atoms are in a mobile state on the surface and, upon forming $^*C(O)$, quickly decompose to form CO. These dynamics are unlikely to describe the processes involved in CO_2 evolution as $-C(O)$ formation has been found to be independent of the O_2 pressure. A Langmuir isotherm, which involves reversible dissociative adsorption of oxygen within the micropores of the catalyst, can, however, explain the observed 0.75 orders (17, 19). In the case of Reaction [4], this adsorption occurs in the vicinity of a $^*C(O_2)$ complex, whereas for Reaction [5] it occurs near the stable $^*C(O)$ surface species. The rate-determining step could then be the adsorption or desorption of O_2 or the rearrangement and subsequent desorption of CO_2.

The activation energy for Reaction [2] of 131 ± 5 kJ $mole^{-1}$ is in agreement with the highest characteristic activation energies calculated by Brown *et al.* (10) for formation of stable surface-oxides $^*C(O)$ on an amorphous carbon. The rate of formation of $^*C(O)$, via Reaction [2], should be equal to the rate of evolution of CO via this reaction step. The magnitude of the characteristic activation energies was determined from the temperature, O_2 pressure, and exposure time and are reported as a distribution of energies ranging from 50 to 140 kJ $mole^{-1}$. The largest values in the range of energies indicate that high O_2 pressures and temperatures combined with long exposure times are required to form the complexes. In the single-site model developed in this paper, a single activation energy for each reaction step is assumed, and the conditions involve relatively high pressures and temperatures so the activation energy for Reaction [2] should correspond most closely to the highest values reported by Brown *et al.* A comparison of the activation energies may not be significant because the earlier study assumes a first-order O_2 dependence, rather than the zero-order dependence determined in the present analysis. The difference in order is related to the type of experiments; Brown *et al.* used isothermal oxidation techniques, whereas in this work TPO is employed. Reported activation energies may differ because of the barriers to O_2 adsorption to and desorption from the carbon surface which must be overcome during isothermal oxidation. In addition, different types and environments of carbon are investigated in the two studies.

For Reaction [3], the optimized activation energy of 36 ± 3 kJ $mole^{-1}$ is difficult to interpret. One possible interpretation of this result is desorption of $^*C(O)$ sites which are adjacent to or which diffuse to active centers such as metal deposits and rapidly desorb. Previous studies on CO desorption from amorphous carbons have determined a distribution of much higher activation energies. For example, Tucker and Mulcahy (20) reported $292 + 80\ (1 - \theta)$ kJ $mole^{-1}$, where θ is the coverage, while Du *et al.* (21) calculated a mean activation energy of 292 kJ $mole^{-1}$ with standard deviation of 33 kJ $mole^{-1}$. Thus a second possibility is that the corresponding small peak predicted in the TPO of catalytic coke could be represented by a distribution of high-energy peaks. A third interpretation is that CO evolution does not proceed via Reaction [3] but is a result of two molecules of carbon monoxide produced from a single molecular oxygen complex with different reactivity to the surface intermediate involved in Reaction [2]; in other words,

$$^*C(O_2) \rightarrow 2CO. \qquad [12]$$

If this is the case, a single-site mechanism is not appropriate, and calculated rate parameters can be, when optimized assuming separate sites and independent of the $^*C(O)$ concentration, similar in magnitude to those listed in Table 1 for Reaction [2]. A detailed analysis of rate parameters associated with Reaction [12] was not carried out because the amount of coke, which corresponds to the difference between the CO produced via Reaction [2] and the CO_2 produced via Reaction [5], is small and not resolved in the TPO profiles. It is not obvious whether these coke species desorb at the high or low temperature ends of the CO curve

or continuously throughout the CO evolution. As a consequence, optimized rate parameters assuming Reaction [12] would have very large errors. In the single-site model, this CO peak is dependent on the $^*C(O)$ concentration and so is constrained to the high temperature end of the observed CO profiles.

The two optimized activation energies for CO_2 evolution of 98 ± 5 and 151 ± 3 kJ mole^{-1} indicate a distinct difference in activity for the two reaction pathways. This observation is in agreement with others who have shown that the presence of $^*C(O)$ complexes retards the combustion rate (22, 23). By assuming that, for both modes of CO_2 formation, the rate-determining step is a rearrangement of the adsorbed species with concomitant CO_2 desorption, then the activation energies reflect the relative stabilities of the intermediates. That is, a complex for Reaction [5], which would consist of three oxygen atoms, is more stable than a complex for Reaction [4], which would consist of an undissociated O_2 and two oxygen atoms. In most cases, it is not possible to compare activation energies reported in the literature on carbon combustion as different mechanisms are often assumed. For example, Ahmed *et al.* (24) proposed a dual-site model and listed three activation energies (270, 150 and 33 kJ mole^{-1}) for three pathways to CO_2 formation. It is not obvious which of these should be compared with our modeled parameters. In addition activation energies would be dependent on whether or not reaction is occurring within the pores of the substrate or on the external surface. Du *et al.* (21) have proposed a similar step to Reaction [4] for evolution of CO_2. They report a single intrinsic activation energy of 119.7 kJ mole^{-1} for this step, which is higher than the 98 ± 5 kJ mole^{-1} listed in Table 1. Tucker and Mulcahy (20) calculated an activation energy of 180 $\pm$ 8 kJ mol^{-1} for steady combustion when oxygen atoms are adsorbed to a graphite surface. This process is equivalent to Reaction [5], but the value we report of 151 ± 3 kJ mol^{-1} is again lower. Taking into account that these reactions are occurring within the pores of the catalyst with intrinsic reaction order of 0.5 then the intrinsic activation energies are 139 and 214 kJ mole^{-1} for Reactions [4] and [5], respectively (25). That is, they are both now higher than reported amorphous carbon combustion energies. This is despite the conclusion by Moljord *et al.* (26) that coke combustion is catalyzed by acidic sites in the vicinity of the coke. However, considering the different experimental and theoretical methodologies required to determine these parameters a ca 15% difference is reasonable.

Kinetic Effects on Structure of TPO Spectra

Figure 4 shows the modeled data for total CO and CO_2 evolution during TPO of highly unsaturated hydrocarbon coke at three different heating rates. Carbon monoxide peaks, for all heating rates, are single symmetric curves. For a single decomposition pathway, rather than the complex competition between four pathways, the peak heights should decrease and the widths broaden with increase in heating rate. The result would be a constant area under the three curves. Peaks heights for CO evolution clearly

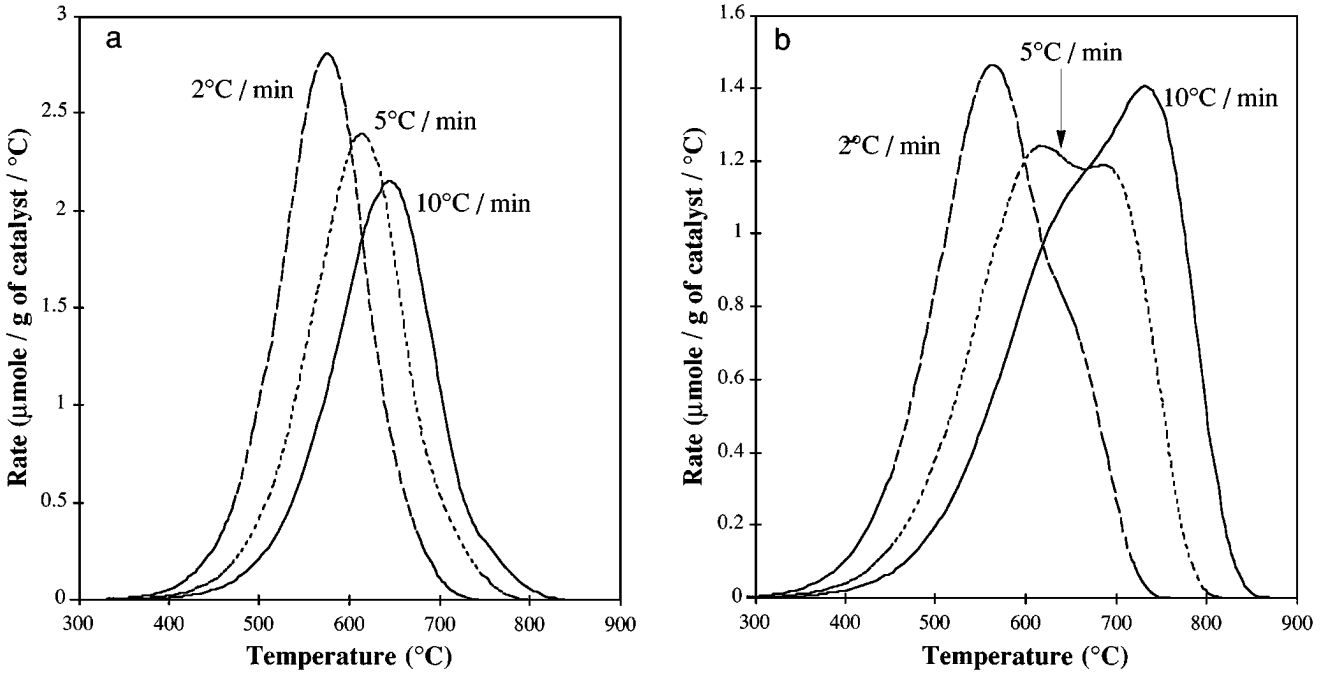

FIG. 4. Heating-rate dependence of simulated evolution rates of (a) CO and (b) CO_2 during TPO of a spent cracking catalyst in 0.939% O_2.

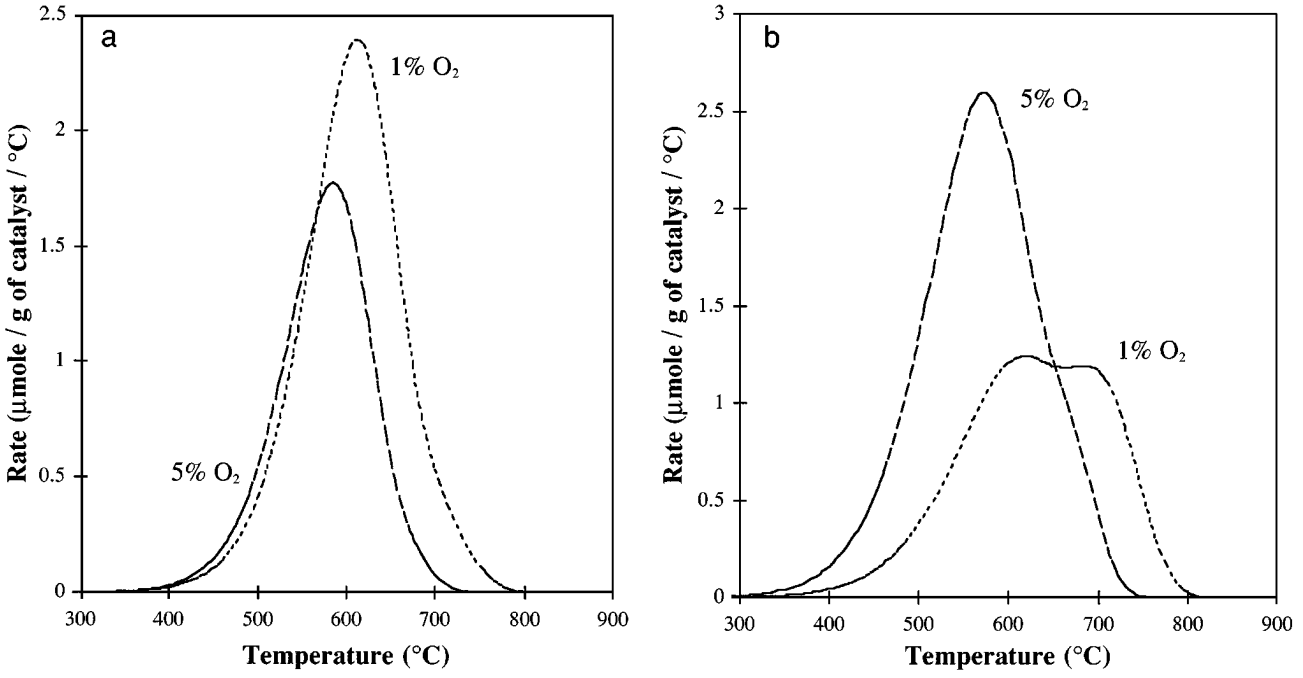

FIG. 5. Oxygen partial-pressure dependence of simulated evolution rates of (a) CO and (b) CO_2 during TPO of a spent cracking catalyst at 5°C/min.

decrease in Fig. 4a but the areas under the curves also decrease. Obviously the CO_2 evolution reactions are competing for carbon sites and are more successful at the higher heating rates. The CO_2 simulated curves shown in Fig. 4b have a more complex structure, with a peak and shoulder for each of the three heating rates. The large first peak at 2°C min^{-1}, which corresponds to Reaction [4], decreases in height as the heating rate increases until it becomes a shoulder at 10°C min^{-1}. At the same time, the small shoulder at 2°C min^{-1}, which corresponds to Reaction [5], increases to a large peak in the 10°C min^{-1} curve.

The effect of O_2 partial pressure is demonstrated in Fig. 5 for CO and CO_2. The CO evolution rate decreases dramatically with increase in percentage oxygen, whereas the opposite is observed for CO_2 formation. This is a reflection of the sensitivity of the competing mechanistic steps to the O_2 reaction order. The 0.75 order for the CO_2 rate compared with the zero order for CO evolution means that at higher O_2 pressures the majority of the carbon is removed by Reaction [4] before the temperature is high enough for Reaction [2] and hence Reactions [3] and [5] to become competitive.

Combined CO and CO_2 evolution profiles at three heating rates for the 0.939% O_2 TPO are shown in Fig. 6. The 2°C min^{-1} curve is symmetric, but at 5°C min^{-1} a small shoulder appears which becomes more distinct at 10°C min^{-1}. Increasing the O_2 partial pressure causes a loss of any structure in the profiles due to the reaction mechanism. Therefore for heating rates greater than or equal to 5°C min^{-1} and for O_2 partial pressures less than or equal to 1% there is a mechanism dependence on the structure of the TPO of coked cracking catalysts. TPO profiles of coke deposited on supported metal catalysts (1, 27) show that all the coke is removed at much lower temperatures (<600°C)

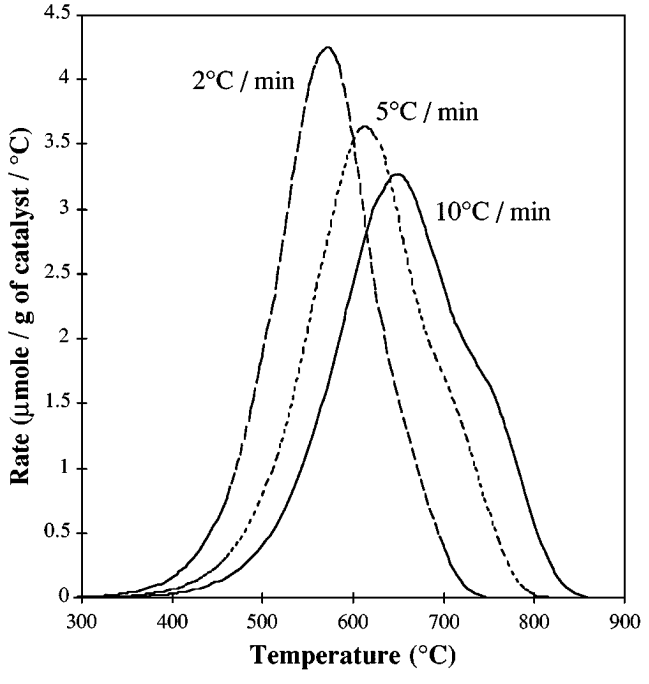

FIG. 6. Heating rate dependence of the combined CO plus CO_2 evolution rates during TPO of a spent cracking catalysts in 0.939% O_2.

than that observed using similar conditions to those reported for cracking catalysts, and that no CO evolution is apparent. Here, only Reaction [4], which would be catalyzed by the metal, is likely to be the dominant process, and structure in the TPO profiles can then be assigned to coke location and type as well as depend on coke particle size and morphology.

CONCLUSIONS

TPO profiles of an industrially spent cracking catalyst were investigated to extract information on the kinetics of catalytic coke combustion. A mechanism for CO and CO_2 evolution was assumed based on four reaction steps and a single type of coke site. Observed peaks and shoulders in the TPO evolved-gas profiles of the high-aromatic coke content of the spent catalysts were then modeled using nonlinear regression. The following conclusions were reached based on this analysis:

i. Two reaction steps for CO formation and two for CO_2 formations provide an excellent simulation to the range of experimental data.

ii. Both rates of CO evolution are independent of the O_2 partial pressure while both rates of CO_2 formation indicate a 0.75-order O_2 dependence. The latter is explained as the rate-determining step being dissociative, reversible adsorption of O_2, but occurring within the micropores of the catalyst.

iii. It is difficult to compare optimized rate parameters with literature values, for each of the reaction steps, because of different proposed mechanisms, techniques, and substrates. However, activation energies for Reactions [2], [4], and [5] compare favorably with reported values on amorphous carbon combustion.

iv. When interpreting TPO evolved-gas profiles of spent cracking catalysts, it is recommended that the linear heating rate be less than $5^{\circ}C\ min^{-1}$ and the O_2 partial pressure be greater than 1%. This should eliminate interference to the structure of the profiles caused by changes in the rate-determining steps.

ACKNOWLEDGMENTS

The authors thank the Australian Research Council for financial support. Financial assistance from a UNERS for CL and from AIDAB for CLM are also gratefully acknowledged.

REFERENCES

1. Querini, C. A., and Fung, S. C., *Appl. Catal. A* **117**, 53 (1994).
2. Le Minh, C., Jones, R. A., Craven, I. E., and Brown, T. C., *Energy & Fuels* **11**, 463 (1997).
3. Haldeman, R. G., and Botty, M. C., *J. Phys. Chem.* **63**, 489 (1959).
4. Weisz, P. B., and Goodwin, R. B., *J. Catal.* **2**, 397 (1963).
5. Weisz, P. B., and Goodwin, R. B., *J. Catal.* **6**, 227 (1966).
6. Massoth, F. E., *I&EC Process Design and Development* **6**, 200 (1967).
7. Massoth, F. E., and Menon, P. G., *I&EC Process Design and Development* **8**, 383 (1969).
8. Magnoux, P., and Guisnet, M., *Appl. Catal.* **38**, 341 (1988).
9. Lear, A. E., Brown, T. C., and Haynes, B. S., *in* "Twenty-Third Symposium (International) on Combustion," p. 1191. The Combustion Institute, Pittsburgh, 1991.
10. Brown, T. C., Lear, A. E., and Haynes, B. S., *in* "Twenty-Fourth Symposium (International) on Combustion," p. 1199. The Combustion Institute, Pittsburgh, 1993.
11. Thomas, J. M., and Thomas, W. J., "Principles and Practice of Heterogeneous Catalysis." New York, VCH, 1997.
12. Redhead, P. A., *Vacuum* **12**, 203 (1962).
13. Le Minh, C., Li, C., and Brown, T. C., *in* "Catalyst Deactivation 1997" (C. H. Bartholomew and G. A. Fuentes, Eds.), p. 383. Elsevier Science, Amsterdam. 1997.
14. Walsh, S., and Diamond, D., *Talanta* **42**, 561 (1995).
15. Billo, E. J., "Excel for Chemists." New York, Wiley-VCH, 1997.
16. Galwey, A. K., *Adv. Catal.* **26**, 247 (1977).
17. Essenhigh, R. H., *in* "Chemistry of Coal Utilisation" (M. A. Elliott, Ed.), p. 1153. Wiley, New York, 1981.
18. Blyholder, G., and Eyring, H., *J. Phys. Chem.* **63**, 1004 (1959).
19. Cheng, A., and Harriott, P., *Carbon* **24**, 143 (1986).
20. Tucker, B. G., and Mulcahy, M. F. R., *Trans. Faraday Soc.* **65**, 274 (1969).
21. Du, Z., Sarofim, A. F., and Longwell, J. P., *Energy & Fuels* **5**, 214 (1991).
22. Laine, N. R., Vastola, F. J., and Walker, P. L., *J. Phys. Chem.* **67**, 2030 (1963).
23. Bonnetain, L., Duval, X., and Letort, M., *in* "Fifth Conference on Carbon." Pergammon Press, New York, 1962.
24. Ahmed, S., Back, M. H., and Roscoe, J. M., *Comb. Flame* **70**, 1 (1987).
25. Levenspiel, O., "Chemical Reaction Engineering." Wiley, New York, 1972.
26. Moljord, K., Magnoux, P., and Guisnet, M., *Catal. Lett.* **25**, 141 (1994).
27. Larsson, M., Hulten, M., Blekkan, E. A., and Anderson, B., *J. Catal.* **164**, 44 (1996).